

Article

Archaeometric Classification of Scattered Marble Fragments to Help the Reconstruction of Statues

Lluís Casas ^{1,*}, Roberta Di Febo ¹, Julio César Ruiz ², Mauro Brillì ³, Fabrizio Antonelli ⁴
and Juan Diego Martín-Martín ⁵

¹ Departament de Geologia, Universitat Autònoma de Barcelona (UAB), Edifici C, 08193 Cerdanyola del Vallès, Catalonia, Spain

² Departament de Ciències de l'Antiguitat i de l'Edat Mitjana, Universitat Autònoma de Barcelona (UAB), Edifici C, 08193 Cerdanyola del Vallès, Catalonia, Spain

³ Istituto di Geologia Ambientale e Geoingegneria (IGAG), Consiglio Nazionale delle Ricerche (CNR), Area della Ricerca di Roma 1, Via Salaria km 29,300, 00015 Montelibretti, Italy

⁴ LAMA–Laboratorio di Analisi Materiali Antichi, Università Iuav di Venezia, San Polo 2468/B, 30125 Venice, Italy

⁵ Departament de Mineralogia, Petrologia i Geologia Aplicada, Facultat de Ciències de la Terra, Universitat de Barcelona (UB), 08028 Barcelona, Catalonia, Spain

* Correspondence: lluis.casas@uab.cat

Abstract: A multi-technique approach combining petrographic, cathodoluminescence, and stable isotope analyses is commonly used in provenance studies of archaeological marbles. In the present paper, this characterization approach transcends provenance, and it is applied to the reconstruction of fragmented sculptures. The potential of this novel application of archaeometric measurements is illustrated with a case study consisting in 16 scattered marble fragments retrieved from a Roman villa (Els Munts) near Tarraco (presently Northeastern Spain). The samples were grouped taking into account their similarity in quantified parameters such as the cathodoluminescence color clusters and the stable carbon and oxygen isotopic ratios. The results permitted classification of the fragments into three groups corresponding to three different statues depicting Antinous (7 fragments), Minerva goddess (4 fragments), and an undetermined character (3 fragments). Two other fragments could not be ascribed to any particular statue. The archaeometric grouping provides arguments that can be used to confirm or refute archaeological hypotheses of statue reconstructions.

Keywords: cathodoluminescence; isotopes; image processing; marble; archaeometry



Citation: Casas, L.; Di Febo, R.; Ruiz, J.C.; Brillì, M.; Antonelli, F.; Martín-Martín, J.D. Archaeometric Classification of Scattered Marble Fragments to Help the Reconstruction of Statues.

Minerals **2022**, *12*, 1614. <https://doi.org/10.3390/min12121614>

Academic Editor: Adrián Durán Benito

Received: 20 November 2022

Accepted: 13 December 2022

Published: 15 December 2022

Publisher's Note: MDPI stays neutral with regard to jurisdictional claims in published maps and institutional affiliations.



Copyright: © 2022 by the authors. Licensee MDPI, Basel, Switzerland. This article is an open access article distributed under the terms and conditions of the Creative Commons Attribution (CC BY) license (<https://creativecommons.org/licenses/by/4.0/>).

1. Introduction

In many civilizations, and particularly in those of the classical world, statues were considered one of the most valued works of art. Often sculpted in marble or other precious stones, they depicted humans, divinities, animals, and mythological creatures.

The earliest Greek statues were placed in temples and represented gods, and by the 7th century BCE, kuroi and korai decorated sanctuaries and gravesites. In classical Greece (5th–4th centuries BCE) the use of statues extended to public and private places including agorae and gateways, the divinities remained the most characterized figures. Later, in the Hellenistic period, statues often portrayed the dynastic leaders and ruler cults included rich victory monuments where nonidealized bodies were also represented.

In the Roman Republic, divinities were also the most depicted subjects in statues, and they were usually exhibited in public places. Naturalistic and nonidealized portraits, often carved as busts, and accompanied with inscriptions were also introduced in public spaces. In Late Republic times, the statues embellished public spaces as fora, temples, basilicas, theaters, and baths. Wealthy people also decorated with statues their gardens and porticoes in cities and country villas. After the conquest of Magna Graecia and later Greece itself, the Romans tried to emulate Hellenistic architectural environments. In imperial Rome, the

emperor official portraits statues and busts were extensively copied and used to highlight their image as a symbol of power. The number of statues in imperial Rome was a feature that had never been seen before. Pieces from the Classical and Hellenistic past were moved to Rome and often copied and adapted.

As a result of the intensive use of stone statues and the durability of the material, it is relatively common to find them in significant archaeological sites. However, it is very rare to find intact pieces. Usually, the bases appear without their corresponding statues. Dispersed and mixed fragments of heads and bodies appear scattered in excavations. Sometimes the statues were even deliberately broken because of iconoclastic expressions. Additionally, the biggest fragments are often found displaced, even reshaped, and reused as building materials. A common problem for archaeologists and restorers is to classify the different fragments and to try to reconstruct art pieces that are in a fragmented status.

The classification and reconstruction of fragmented statues is an arduous task usually undertaken by manually checking matching pairs. Digitalization of the fragments through 3D scanning can be helpful to attempt virtual reconstructions and to check virtually different reconstructive hypotheses [1,2] including the addition of missing or incomplete fragments. Artificial intelligence algorithms can also be used to compute automatically the most probable positions of the fragments [3]. These automatic methods often allow the setting of a flexible set of operators by the user that can result in highly plausible reconstructions. However, before attempting any manual or computer-assisted reconstruction, it is crucial to know, with the highest possible certainty, that the fragments under study do really belong to the same object. Several archaeometric approaches have the potential to shed light into this issue, but as far as we know, they have only been rarely used to confirm or refute archaeological reconstruction hypotheses [4].

In the case of marble statues, the common archaeometric characterization techniques include petrography, stable isotope studies, and cathodoluminescence. However, this characterization is usually aimed at unveiling the provenance of the marble [5–7], and this essentially to obtain information on the chronology, the importance of the piece, the financial status of the owners, the economic relations, or the ancient commercial routes. Archaeometric characterization is not commonly used to discern the fragments that belong to the different statues retrieved from a given site because often many of them are carved using the same marble variety. For instance, in a provenance study of marbles from the Hadrian's Villa, the prevalence of Carrara marble was observed [8]. Similarly, in a study of Roman marble sculptures from the National Museum of Carthage [9], nine out of thirteen statues were carved in Pentelic marble. Usually, it is assumed that the archaeometric discrimination between fragments of two statues worked in a same variety of marble is not possible.

In this paper, we illustrate this possibility with a set of 16 fragments of marble retrieved from the Roman villa of Els Munts (12 km from Tarragona, Northeastern Spain), some of them assigned to a portrait of Antinous and others to a statue of Minerva. The common multi-technique archaeometric characterization was applied to all the fragments to infer their provenance. Once established that most of the fragments could belong to a same marble variety, the quantification of the cathodoluminescent (CL) colors and stable isotopes were used to add objective and numeric data to the archaeological discussions and open hypotheses on statue reconstructions. The main goal of the investigation is to find archaeometric evidence to distinguish fragments from different statues and ultimately to determine the identity of the fragments to either the Antinous portrait or the goddess Minerva statues.

Recently, this classification approach has been effectively applied to check some reconstruction hypotheses of the Forma Urbis Romae [10]. Both CL response and isotopic signature can be sometimes characteristic of a given variety of marble, but there are always slight variations (in CL color, CL intensity, CL distribution, and isotopic ratios). The approach presented here assumes that CL and isotopic measurements from a single carved object should produce more similar CL features and isotopic values compared to fragments from other objects, even in the case of statues carved with the same marble variety. This

hypothesis had been proven correct for physically matching slab fragments from the Forma Urbis map [10]. The importance of reconstruction, in the case of fragmented statues and generally for any type of sculpture, concerns many aspects of significance to archaeologists, art historians, historians, and museum conservators, such as the preservation of the knowledge gathered on the artwork, its functional (e.g., decorative, devotional, memorial) and economic contexts or the present-day value of the preserved object.

2. Materials and Methods

2.1. Sampled Materials

The sampled materials are marble statues and fragments (Figure 1) from the Roman villa known as “Els Munts” (in Altafulla, Catalonia, Northeastern Spain) [11]. This villa was built in the 1st century CE on a hill 12 km east from Tarraco (presently Tarragona) along the coast. The villa outstands for the size of the archaeological site and the sumptuousness of its decorative elements. During the 2nd century CE, its splendor was at its peak, it was the residence of Caius Valerius Avitus, one of the duumvirs of Tarraco. At the end of the 3rd century, a great fire destroyed most of the villa, although it remained partially occupied until the 6th or 7th century. Abundant material was excavated from the site, including elements of the decorative program of the building, among this, a large quantity of statues. The better-preserved free-standing statues have been intensely studied, mainly by Koppel [12,13].

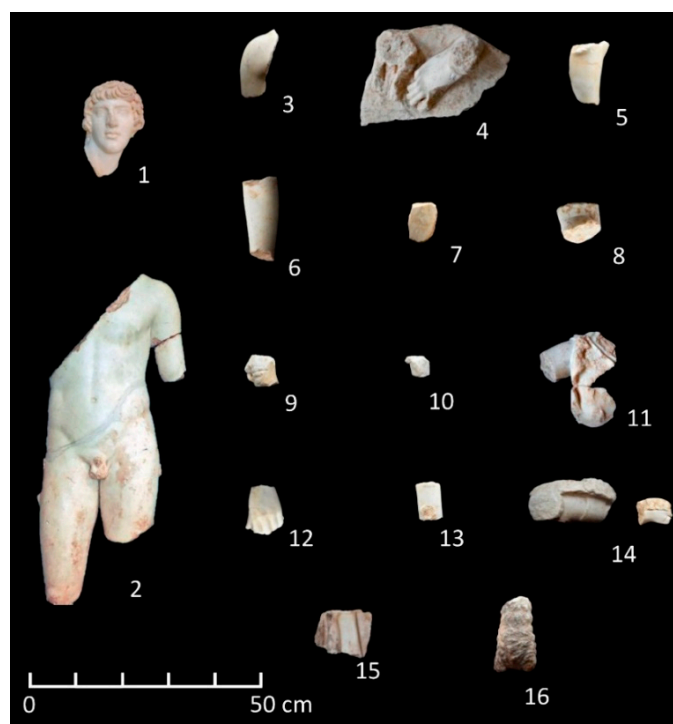


Figure 1. The sixteen sampled marble fragments retrieved from the “Els Munts” Roman villa.

Apart from the well-studied statues, many more fragments have remained unstudied in the off-site collections of the Museu Nacional Arqueològic de Tarragona (MNAT) since the excavations undertaken in the sixties of the last century. The study of these unpublished statues is currently being undertaken by one of us (J.C.R.) and some preliminary conclusions have been drawn [14]. Most of these fragments were found in the residential building of the villa around the ambulatory and the rooms of representation where guests were received. Possibly, the corresponding statues were part of the decorations in these areas. Despite their fragmentary state, it is occasionally possible to identify mythological and divinity representations, mainly of small size and rarely with sizes above the natural size.

A total number of 16 marble fragments (Figure 1 and Table 1) were carefully collected from fracture surfaces in the form of tiny chips using a small hammer and a chisel, avoiding

weathered material and patinas. All the samples were split into two parts, one to be used for thin-section preparation, the other one to be pulverized for isotopic analysis. In two cases (samples 11 and 12), the sampled fragment was too small to split, and the whole fragment was ground.

Table 1. Sampled marble fragments, with indication of museum and excavation references, a short description, the context where they were found, and the year of the finding, along with the most accepted archaeological interpretation about their identity.

Label	MNAT Ref.	Excavation Ref.	Description	Context (Year)	Archaeological Hypothesis
1	45406	-	Antinous head	RB ¹ , cistern (1969)	Antinous
2	45406	-	Antinous torso	RB ¹ , corridor (1995–1996)	Antinous
3	-	-	Right shoulder	unknown (1960–1970)	Antinous?
4	46589	EM-96-4501-1	Pedestal with right foot and animal legs	RB ¹ , room 4500, UE 4501 (1996)	Antinous?
5	-	EM-1969	Undetermined anatomical fragment (leg?)	RB ¹ . Last room in northern corridor, layer III (1969)	Antinous?
6	-	EM-96-4601-1	Arm fragment	RB ¹ . Room 4600, UE 4601 (1996)	Antinous?
7	-	-	Forearm fragment?	RB ¹ . Last room in northern corridor, layer III (1969)	-
8	-	-	Knee fragment	unknown (1960–1970)	Antinous?
9	-	-	Forearm fragment? with indetermined attribute	unknown (1960–1970)	-
10	-	EM-95-4108-20bis	<i>Puntello</i> fragment	RB ¹ . Corridor, UE 4108 (1995)	-
11	-	EM-95-4108-4/EM-96-4310	Right-top part of a torso of a statue with aegis (split in two fragments)	RB ¹ . Corridor, UE 4108 (1995) and Room 4300, UE 4310 (1996)	Minerva?
12	-	EM-95-4108-5	Left hand with undetermined object	RB ¹ . Corridor, UE 4108 (1995)	Antinous?
13	-	EM-95-4102-14	Right forearm fragment? includes <i>puntello</i>	RB ¹ . Corridor, UE 4102 (1995)	Antinous?
14	46558	EM-96-4306-1	Fragment of forearm and hand with shield (split in two fragments)	RB ¹ ‘Stuccos trench’ (1968) and Room 4300, UE 4310 (1996)	Minerva?
15	-	EM-96-4511-1	Statue dressed in peplos?	RB ¹ , room 4500, UE 4511 (1996)	Minerva?
16	-	-	Body fragment of an indetermined animal	Presumably from the RB ¹ . Corridor, UE 4102 (1995)	Minerva?

¹ Residential building.

The sampling criterion was driven by the macroscopic similarity between the sampled marble fragments and two pieces on display at the Costa dock exhibition facilities of the MNAT. These two pieces were also sampled (samples 1 and 2) and consist of an isolated head and a torso stuck with part of the extremities (Figure 1). The portrait is interpreted to depict Antinous, a Greek youth and favorite of the Roman emperor Hadrian, which was deified after his premature death. This Antinous portrait is the only one reported in Hispania and one of the few found in a private villa. The surfaces of the sampled fragments do not match with the fracture surfaces of the head and body of Antinous and all evidence indicates that the statue was shattered in very many pieces.

The only previous provenance study on this statue is from the eighties of the last century and restricted to the head. A Paros origin was suggested for its marble exclusively by petrographic thin-section examination [15]. Unfortunately, no contrastable graphic material is available in the mentioned reference. Therefore, the present study can be considered the first provenance study of the marble fragments from the “Els Munts” villa. Taking into account the exceptional nature of the sculpture repertoire of this villa, some years ago, Pensabene [16] already pointed out the need for a full review of its carved marbles, including the Antinous head. The torso, found in the nineties of the last century, does not connect directly with the head, but considering their characteristics, were already assigned to the same statue by Koppel [12]. However, so far, no archaeometric study has been done to corroborate this ascription. Additionally, after a careful systematic revision of the statues and fragments from the off-site collections of MNAT, we suggest the ascription of seven fragments (labels 3, 4, 5, 6, 8, 12, and 13 in Table 1) to the Antinous statue. This attribution is based on consistent proportions, similar surface finish, and analogous macroscopic aspect of the marble.

Another group of sampled marble fragments (those labeled 11, 14, 15, and 16) also share macroscopic features with the portrait of Antinous. However, based on iconographic grounds, this group seems to belong to another statue, perhaps depicting goddess Minerva. One of these fragments, a left forearm and hand with shield (label 14), was arbitrarily interpreted as a part of a gladiator statue supposedly corresponding to the decoration of the baths of the villa [12]. Finally, three more fragments (7, 9, and 10) were also sampled and there is not any archaeological interpretation for them.

2.2. Methods

At the Istituto di Geologia Ambientale e Geoingegneria (CNR) of Rome, oxygen and carbon isotopic ratios were determined on all the sampled fragments using a small amount (0.15–0.20 mg) of powdered marble. A Thermo Gasbench II automatic preparation device was used for phosphoric acid digestion at 72 °C and CO₂ purification; a Finnigan Delta Plus mass spectrometer measured the ¹³C/¹²C and ¹⁸O/¹⁶O isotope ratios of the carbon dioxide produced from the digested marble powder. The results were expressed in the usual delta notation, which represents the relative deviation in parts per thousand of the heavy isotope/light isotope ratio of the samples from that of a reference standard. The international standard used was V-PDB for both the oxygen and carbon isotopes. The precision of the analyses was ±0.10‰ (1σ) as observed from repeated analysis of three in-house calcite standards.

Petrographic thin-sections were prepared from the largest samples extracted from the sampled fragments. These were characterized petrographically using a polarizing light microscope (OM) (Nikon Eclipse E600 POL, Tokyo, Japan) under plane polarized light (PPL) and cross polarized light (XPL). The thin-sections were also observed under cathodoluminescence (CL) microscopy at the Earth Sciences Faculty, Universitat de Barcelona, using CL8200 Mk5-1 equipment (Cambridge Image Technology Ltd., Welwyn Garden City, Hertfordshire, UK), with operating conditions of 15 kV and a gun current of ~300 μA. Images were obtained with exposures time of 3, 6, and 15 s for all the analyzed areas. Numerically quantifiable petrographic parameters (MGS, MFS) were measured using NIS-Elements, Microscope Imaging Software (Nikon, Tokyo, Japan).

The obtained cathodoluminescent images were treated statistically to quantify their color features in order to establish similarities between samples. The CL images were first cropped to isolate large rectangular areas containing only the colors of the CL response of samples (cracks, empty spaces, and adjacent areas to the marble thin-section were avoided). Average pixel values were computed for all of the images. Additionally, pixel clustering was also applied to the cropped images using the CLARA algorithm [17]. After clustering, the images were transformed into a segmented (or simplified) version of them containing only a limited number of different colors (from 1 to 10). The values corresponding to the average pixels and color clusters were numerically expressed as RGB triplets indicating the combination of red (R), green (G), and blue (B). As RGB is an additive color model, white

is represented by (255, 255, 255) and black by (0, 0, 0). To represent the color values in a bidimensional plot, the color CIE 1931 xy chromaticity diagram was used. In addition to the quantification of the colors, the size of every CL color cluster was also quantified with a numerical value indicating the corresponding number of pixels of the cluster.

3. Results

3.1. Petrography

The petrographic features of all the analyzed marbles are summarized in Table 2. The microscopic study showed calcite marbles with isotropic fabric and, generally, heteroblastic microstructure (sample 5 is the only with a homeoblastic one) forming a mosaic of crystals (Figure 2). See Figure S1 within the Supplementary Materials for illustrative micrographs of all the analyzed samples. Occasionally the crystals define a mortar-like microstructure consisting of larger crystals surrounded by smaller crystals instead of strictly defining a mosaic (sample 3 and, to a lesser extent, sample 7). The maximum grain size (MGS) values are generally above 2 mm. The coarser sample is number 8 with an MGS of 2.64 mm. Only three samples show values below 2 mm (samples 5, 10, and 14) and these would correspond to fine-grained marbles. However, especially in the case of sample 10, the total surface useful for obtaining a thin-section was very small. Therefore, it is not possible to exclude coarser grain-size marbles. Besides MGS, the most common grain size is generally between 0.6 and 1.5 mm (for sample 14 the most common values are between 0.5 and 0.6 mm). The shape of the boundaries between grains are invariably curved and often embayed. Finally, another common feature generally observed in the analyzed samples is the presence of straight mechanical twinning in the crystals in the form of thin twins (type I) and tabular thick twins (type II) [18]. In most of the cases (9 samples out of 14; see Table 2), the petrographic features observed using the optical microscope fit well with those recognized for the Parian marbles (Greece), particularly the variety quarried in the Lakkoi district (Paros-2). Samples 3, 7, 10, and 14 could also probably be associated with Parian marble, but they show some disharmonious attributes. On the one hand, sample 7 and in particular sample 3 exhibit a mosaic microstructure tending to mortar that does not allow ruling out a provenance from Prokonnesos (presently Marmara Island, Turkey); on the other hand, should samples 10 and 14 be really fine-grained, they would be classified as Pentelic (Attica, Greece). Finally, sample 5 is most likely a fine-grained marble with microstructural features compatible with marmor Lunense (presently Carrara, Apuan Alps, Italy), although a provenance from Göktepe (Ephesos, Asia Minor) cannot be excluded.

Table 2. List of the main petrographic characteristics and isotopic ratios (V-PDB ‰) corresponding to the measured samples. Textural qualifiers are Hom: homogeneous; Het = heterogeneous; Mor = mortar; Mot = mottled; Bo = boundary grains; MGS is maximum grain size; MFS is most frequent grain size range. GBS is grain boundary shape, C = curved or E = embayed. CL is cathodoluminescence; LL (very low)/L (low)/M (medium).

Sample	Texture	MGS (mm)	MFS (mm)	GBS	CL Intensity	CL Texture	$\delta^{13}\text{C}$ (‰)	$\delta^{18}\text{O}$ (‰)	Hypothesized Provenance
1	Het/Mos	2.08	0.6–1.2	C	LL	Hom	2.34	−3.14	Paros-2
2	Het/Mos	2.16	0.5–1.5	C	LL	Hom	2.33	−3.20	Paros-2
3	Het/Mor	2.56	0.7–1.2	E/C	LL	Hom	2.39	−3.07	Paros-2/Prokonnesos
4	Het/Mos	2.40	0.6–1.0	C/E	LL	Het/Mot	1.65	−3.43	Paros-2
5	Hom/Mos	1.72	0.7–1.3	C	M-L	Het	2.07	−3.17	Carrara/Göktepe
6 ¹	-	2.00	-	-	LL	Hom	2.18	−3.28	Paros-2
7	Het/Mos to Mor	2.40	0.8–1.4	C/E	LL	Hom	1.91	−3.25	Paros-2/Prokonnesos
8	Het/Mos	2.64	0.8–1.7	C/E	LL	Het/Mot	1.26	−3.99	Paros-2
9	Het/Mos	2.16	0.8–1.4	C/E	LL	Het/Mot	1.92	−3.61	Paros-2
10 ¹	Het/Mos	1.26	0.5–1.0	C/E	LL	Het/Mot	2.13	−4.03	Paros-2/Pentelikon?
11	Het/Mos	2.32	0.8–1.2	C/E	LL	Het	2.36	−3.61	Paros-2
12 ²	-	-	-	-	-	-	2.13	−3.66	Paros-2
13 ²	-	-	-	-	-	-	2.21	−3.52	Paros-2
14 ¹	Het/Mos	1.28	0.5–0.6	C	LL	Het/Bo	1.93	−4.68	Paros-2/Pentelikon?
15	Het/Mos	2.56	0.7–1.7	C	LL	Het/Bo	2.14	−4.89	Paros-2
16	Het/Mos	2.48	0.6–1.5	C/E	LL	Het	1.26	−3.60	Paros-2

¹ The area cut in the thin-section is not (6) or may not (10, 14) be statistically significant; ² No thin-section was cut.

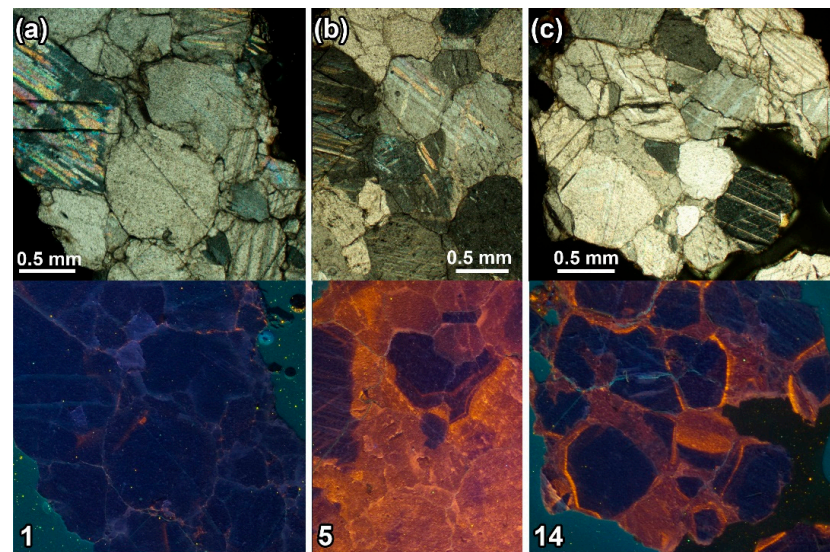


Figure 2. Petrographic images of three representative sampled marble fragments including XPL (top) and CL (bottom) micrographs of the same areas using an exposure time of 15 s. (a) sample 1; (b) sample 5; (c) sample 14.

3.2. Stable Isotopes

The results of the measured stable C and O isotope ratios corresponding to the 16 sampled marble fragments are summarized in Table 2. The isotopic values are rather similar and range from 1.26‰ to 2.39‰ for carbon ($\delta^{13}\text{C}$) and from -3.07 ‰ to 4.89‰ for oxygen ($\delta^{18}\text{O}$).

All the isotopic values are plotted in a diagram in which the isotopic fields of the main medium/coarse-grained classical white marbles [19] are represented together with a relevant Hispanic marble after [20] (Figure 3). Considering the MGS values, all the samples (except 5, 10, and 14) can be unquestionably represented in this diagram. Almost all the samples lie in an area where five different fields overlap; these are Aphrodisias, Paros-2, Prokonnesos-1, Naxos, and Hispanic Macael marbles. However, an Aphrodisian and Naxian origin can be certainly ruled out by considering the petrographic features described above.

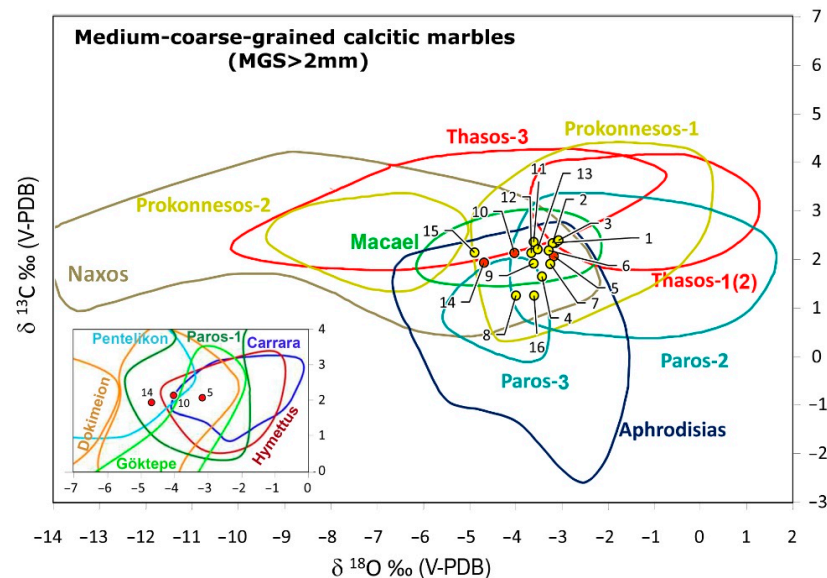


Figure 3. Isotopic results from the analyzed samples plot with the isotopic reference isotopic fields for medium/coarse-grained classical marbles from [19]. Macael reference field from [20] is also included. In an inset plot, samples with $\text{MGS} < 2$ (red dots) are also represented with respect to the fine-grained isotopic diagram proposed by [19].

Strictly speaking, samples 14 and 15 are actually outside the Paros-2 field and samples 8 and 16 are outside the Macael domain.

Plotting the three samples with MGS < 2 mm in the isotopic diagram proposed by [19] for fine-grained classical marbles, they appear in an area covered by many isotopic fields, including those corresponding to the marbles of Carrara, Göktepe, Paros, and Pentelikon.

3.3. Cathodoluminescence

3.3.1. CL Facies

The CL signal measured in petrographic thin-sections is commonly described qualitatively in terms of color, intensity, and homogeneity [20]. In general, all the studied samples show a very low intensity cathodoluminescence (CL) with blue/violet hue (see Table 2 and Figure 2a), the only exception is sample 5. In contrast with the other samples, sample 5 exhibits an orange medium-intensity CL with some small patches of very low blue/violet hue (Figure 2b). See Figure S2 within the Supplementary Materials for illustrative micrographs of all the analyzed samples viewed under the CL microscope.

Regarding the distribution of the CL, it varies from relatively homogeneous (samples 1, 2, 3, 6, and 7) to clearly heterogeneous (samples 4, 5, 8, 9, 10, 11, and 14). Specifically, for the medium-intensity CL of sample 5, the orange CL surrounds certain relict crystals bearing almost no CL signal or very low violet (Figure 2b). Similarly, for some samples, such as 11, 14, and 15, the orange CL isolates crystals of very low CL but in contrast, the orange areas are marginal compared with the grains of very low CL (Figure 2c). Finally, other samples, such as 4, 8, and 10, the areas of orange CL are even scarcer and often limited to small veins.

It is known that for marbles and limestones, the low wavelength CL emission (blue/violet) is due to intrinsic luminescence centers, mainly lattice imperfections [21]. In contrast, the higher wavelength emission (orange/red) is due to extrinsic luminescence centers due to the presence of CL-activator impurities, mainly Mn^{2+} replacing Ca^{2+} in calcite [22]. However, the role of impurities is very complex as there are other reported activator elements as well as inhibitors, and they can interact, thus modifying the overall luminescence response [23,24]. Considering the predominance of the intrinsic CL response for most of the samples (except sample 5), from the marble provenances suggested by the isotopic values (Figure 3), the Naxian provenance can be definitely excluded because its archaeological marbles belong to the orange CL family [25,26]. The Hispanic provenance (Macael) is also implausible because its rare lithotypes with relict grains of low-intensity CL always exhibit very high intensity orange/yellow CL limits [27]. The other three suggested provenances (Aphrodisias, Paros-2, and Prokonnesos-1) are indeed among the blue CL family, but it is difficult to decide which is the most plausible origin. On the one hand, these three marbles generally present a homogeneously blue/violet CL without orange CL patches. However, according to the results shown in [28], Paros-2 is the only marble that appears to present a certain CL heterogeneity but with an overall medium CL intensity and not low intensity.

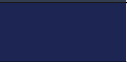
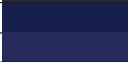
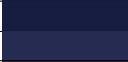
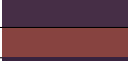
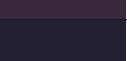
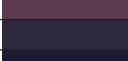
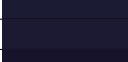
The fine-grained samples studied (5, 10, and 14) are among those with clearly heterogeneous CL, which again complicates their identification with known CL facies. Nevertheless, some classical fine-grained marbles that commonly display homogeneous low-intensity CL are also known to occasionally exhibit combinations of low-intensity (dark or blue) and medium-intensity (orange) domains, such as Göktepe, where small orange domains can sometimes appear [29] and Carrara, where small dark domains can infrequently appear [30]. Another well-known fine-grained marble, Pentelikon, exhibits a heterogeneous CL but always including very high-intensity orange CL domains [28,31] not observed in any of the analyzed samples. This questions the ascription of samples 10 and 14 to a Pentelic marble.

3.3.2. CL Color Clustering

The CL images treated with the CLARA algorithm turned into simplified versions of them bearing a limited number of colors. The algorithm was set to allow ten as the maximum number of colors. However, most of the simplified images contain only two colors (see Table 3). The images corresponding to samples 4, 8, 9, and 16 contain three

color clusters, and sample 11 is the exception to this reduced number of color clusters as its corresponding image contains eight different colors (although actually three of them with a rather low number of pixels). See Figure S3 within the Supplementary Materials for the cropped CL image areas and their corresponding simplified versions.

Table 3. RGB color values for the analyzed CL images including the average pixel and the color clusters for the images treated with the CLARA algorithm; the area percentages of the color clusters are also indicated. The actual colors are also reproduced.

Sample	Average Pixel			Color	Number of Clusters	Color Clusters				
	R	G	B			%	R	G	B	Color
1	28	34	67		2	55	22	28	62	
						45	32	38	72	
2	29	38	82		2	62	23	31	77	
						38	37	43	91	
3	27	32	68		2	75	23	29	65	
						25	38	43	81	
4	42	33	59		3	47	46	34	58	
						37	24	25	55	
						15	70	46	70	
5	113	60	60		2	70	135	67	64	
						30	55	35	62	
6	30	35	63		2	62	24	31	59	
						38	35	42	70	
7	14	28	66		2	65	20	35	74	
						35	11	25	62	
8	58	44	66		3	42	56	43	63	
						33	79	52	71	
						25	28	29	60	
9	58	41	60		3	43	42	30	52	
						43	64	45	64	
						14	92	59	80	
10	35	31	52		2	65	45	40	60	
						35	27	27	51	
						32	28	26	50	
						22	23	19	42	
11	34	26	47		8	12	35	32	54	
						12	36	28	43	
						10	46	29	47	
						5	62	40	52	
						4	43	42	60	
						3	76	49	56	
14	55	39	55		2	62	87	51	55	
						38	31	31	57	
15	49	40	60		2	63	71	49	70	
						37	30	31	59	
16	34	31	57		3	51	57	48	67	
						36	42	32	57	
						12	25	26	57	

The RGB values obtained were converted into CIE XYZ values. These latter values characteristically have very low Y (luminance) values. In fact, except the most reddish color cluster of sample 5, luminances are always below 5 (in the 0–100 range). The XYZ values were then converted into xy values to plot them on a bidimensional luminance-independent chromaticity diagram [32]. The results are shown in Figure 4.

The values corresponding to the color clusters align roughly in a slightly curved line within the chromaticity plot, in a color area that ranges from the blue-violet color region toward the purple, yellowish pink, and orange regions. The corresponding average pixels for all the samples also align within the same curved line.

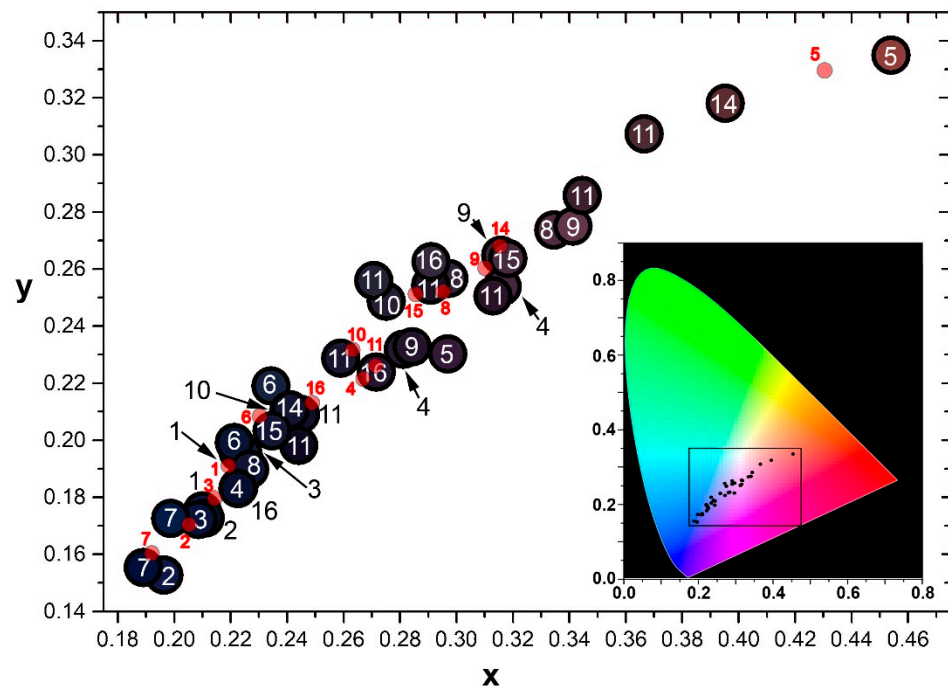


Figure 4. Position of the color clusters in an xy chromaticity diagram with indication of the corresponding sample. The position of the average pixels for all the images is also represented in red. Inset: A colored complete chromaticity diagram with indication of the color cluster position (black dots) and the rectangle corresponding to the part of the diagram depicted in the main figure.

4. Discussion

The first requirement to start a possible reconstruction of a fragmented statue is obviously that all the fragments considered belong to the same type of marble. The petrographic results indicate that most of the analyzed samples indeed show similar microstructural features (isotropic fabric, curved to embayed grain boundaries, and more or less comparable MGS and MFS values). The CL response is also similar for most of the samples, with predominance of low-intensity blue/violet colors with a secondary role (sometimes almost inexistent) of orange CL color in some small areas. Most of the sampled marbles were identified as the medium-grained marble Paros-2. However, samples 3 and 7 are not so straightforward identified as Paros-2, and an origin from Prokonnesos is also plausible. Additionally, samples 10 and 14 appear as fine-grained marbles petrographically consistent with Pentelikon origin, although the observed CL casts doubt on such interpretation. However, the small area cut in the thin-section of these two samples might not be statistically significant, if both marbles were actually medium-grained they would also be classified as Paros-2. In contrast, there is no doubt on the fine-grained condition of the homeoblastic marble from sample 5, and it definitely cannot be classified as Paros-2. Its petrographic characteristics and the predominance of medium-intensity orange CL with low-intensity blue CL patches make Carrara (or Göktepe) plausible adscriptions. Furthermore, it should be noted that the volumes of samples labeled 12 and 13 did not permit cutting them as thin-sections.

Apart from sample 5 (and with some doubts on samples 3, 7, 10, and 14) it is reasonable to undertake a classification of the samples according to their CL similarity to assign them to different statues. In the reconstruction of the slabs from the Forma Urbis Romae [10], a similar kind of classification was performed by measuring the similarity between marble fragments based on averaged CL colors. In the present case, the averaged pixels concentrate in a very short segment and the discussion on the similarity between samples has been articulated using essentially the results from pixel clustering, and the averaged pixel values are only considered tangentially.

Only two samples are undisputedly assigned to a given statue (samples 1 and 2). These two samples belong to the head and torso of the so-called Antinous statue, on display at the Costa dock exhibition facilities of the MNAT. Both samples exhibit similar average colors with low x and y chromaticity coordinates and their corresponding segmented images contain only two color clusters, again with similar chromatic coordinates (Figure 5). In fact, one of the color clusters is essentially the same for both samples. Apart from these two samples, there are three other samples (3, 6, and 7) with similar chromatic values (Figure 5, red circles). All these samples are characterized by an almost complete absence of orange patches of CL and their corresponding fragments could belong to the same statue, and the others would not be part of the Antinous statue.

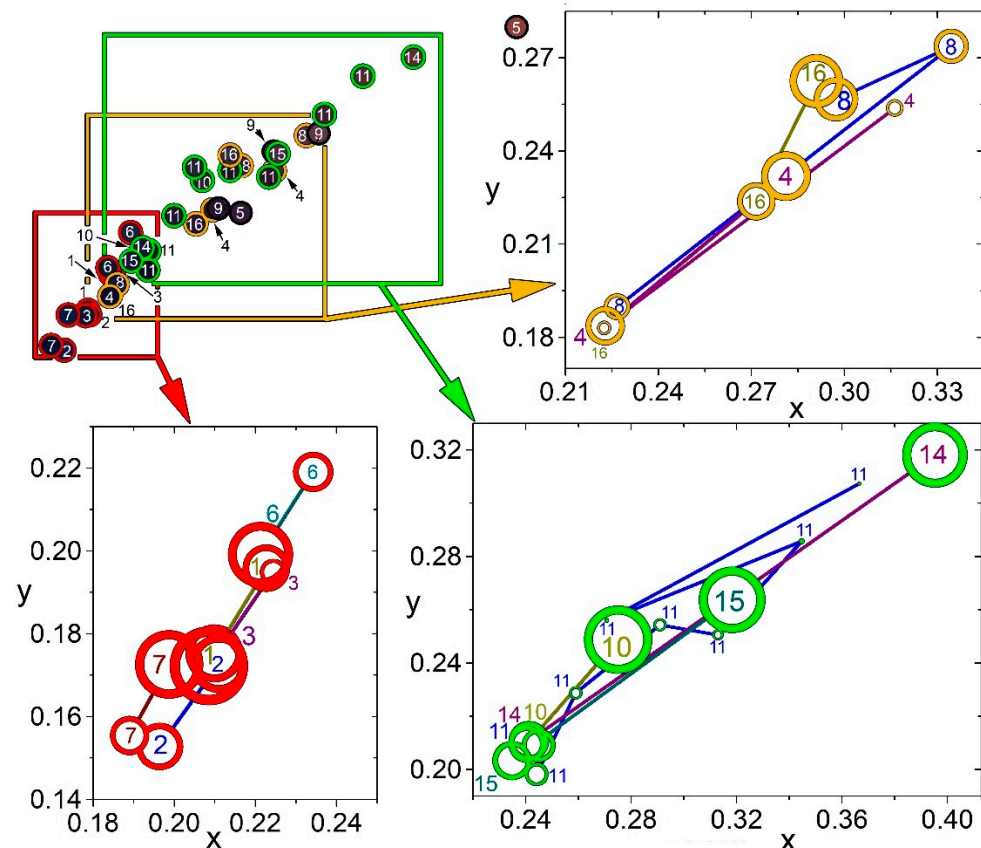


Figure 5. The color clusters position (open dots) as depicted in Figure 4, but now grouped and zoomed in three sets (red, green, and yellow) to highlight the chromatic similarities between the CL response of the different samples. The size of the open dots in the zoomed sets has been made proportional to the size of the corresponding color cluster.

The individuation of samples with absence of orange CL patches was already rather noticeable without the use of tools to quantify the CL colors. For the rest of the samples, a qualitative classification would not produce straightforward results and quantification appears to be more necessary. One of the samples (14) comes from a fragment of forearm and hand with shield—this suggests a possible Minerva statue. The corresponding cathodoluminescence facies for this sample contain bluish CL relict-grains surrounded by more intense orange CL areas (Figure 2c). A way to select other similar samples would be to focus on the bluish relicts using the color clusters from the segmented images. There are three other samples (10, 11, and 15) that have approximately a blue color cluster located at the same coordinates (Figure 5, green circles). The corresponding fragments could thus belong to the statue depicting, presumably, Minerva.

From the remaining samples, a group of three (4, 8, and 16) emerge. For this group, the color classification produced three different clusters and again they share coordinates for

the corresponding blue cluster and exhibit a certain affinity regarding the other two color clusters (Figure 5, yellow circles). Therefore, the three samples could hypothetically be part of the same statue. Finally, the CL features of sample 9 (and obviously also sample 5) remain ungrouped and this lack of affinity with other samples suggests that they are not part of any of the three statues. This inference was already clear for sample 5 because petrographically it was unquestionably assigned to a different type of marble.

It is worth noting that the isotopic data support the suggested classification of the analyzed fragments in three groups (Figure 6). The samples of Antinous' fragments (1, 2) exhibit the highest isotopic ratios ($\delta^{18}\text{O}$ and $\delta^{13}\text{C}$) and group together with the samples that are also attributed to this sculpture, shown in the upper-left corner of the plot. Fragments 12 and 13, which could not be analyzed by cathodoluminescence, also archaeologically attributed to the Antinous statue, locate reasonably close to this group of samples and therefore the archaeological attribution is also supported archaeometrically. The fragment that is seemingly part of a Minerva statue exhibits lower $\delta^{18}\text{O}$ ratios that align with the other three fragments associated to this statue, plotting within a narrow band of $\delta^{13}\text{C}$ values (green dots in Figure 6). The third group of samples that emerged according to the classification obtained from the CL analyses (4, 8, and 16) also appears grouped within the isotopic plot exhibiting the lowest $\delta^{13}\text{C}$ values (yellow dots in Figure 6). Finally, the isotopic ratios of the isolated samples 9 and 5 appear rather close to the ratios produced by the samples attributed to the Antinous. However, a hypothetical connection of these two fragments to the Antinous statue appears almost certainly impossible for sample 5 and rather unlikely for sample 9. On the one hand, both samples exhibit clearly visible orange (or rather purple for sample 9) CL patches that are completely absent in samples attributed to the Antinous statue; on the other hand, sample 5 is petrographically different from the samples attributed to this statue.

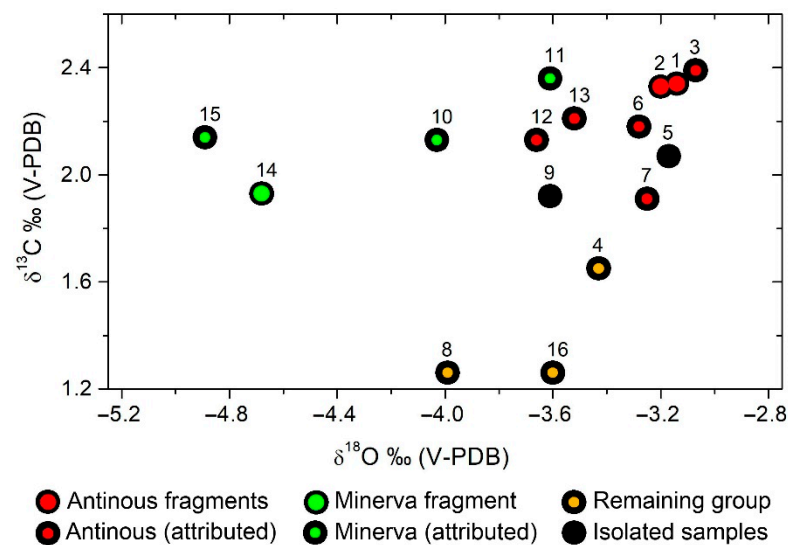


Figure 6. Detail of the isotopic results shown in Figure 3, here coloring the samples according to discussed attributions. Black dots correspond to samples of fragments not linked to any other fragment.

5. Conclusions

The archaeometric provenance study of the 16 studied marble fragments points to a shared marble variety for 11 of them, most probably Paros-2. Additionally, four other samples (labeled 3, 7, 10, and 14) might also have this same provenance despite showing some unusual characteristics for a Paros-2 marble (the mortar microstructures of samples 3 and 7 suggest alternatively an origin from Prokonnesos; samples 10 and 14 exhibit lower grain-size than expected). One of the studied marble fragments (labeled 5) is certainly not a Paros-2 marble and Carrara (or Göktepe) appears as the most reasonable provenance.

In addition to their contribution in the multi-technique approach commonly used in provenance studies, the combination of isotopic and cathodoluminescence measurements has proven to be a successful approach to classify marbles of a given variety into groups to be correlated with different statues. The presented approach brings archaeometric arguments that can contribute to confirm or refute archaeological hypotheses of statue reconstructions.

Most of the 16 analyzed fragments that were included in this case study could be archaeometrically grouped into three sets attributed to statues depicting young Antinous (7 fragments), Minerva goddess (4 fragments), and an indetermined character (3 fragments). Two fragments were not assigned to any set and they would belong, separately, to other statues. The archaeometric study confirmed that the Antinous head (label 1) and the torso (label 2) are indeed part of a same statue along with most of the fragments initially ascribed to it and additionally fragments labeled 7 and 10. However, some doubts remain for these two fragments and from the petrographic point of view, on the true adscription to Paros-2 marble and therefore also to the Antinous statue. From the fragments initially ascribed to the Antinous, only the fragments labeled 5, 4, and 8 were finally not attributed to it. The last two, along with fragment 16 (initially related to the Minerva statue), were considered to be part of a different statue. Concerning fragment 5, CL (and petrographic) data strongly suggests that is made of a different type of marble and, together with sample labeled 9, are the only two fragments that could not be linked to any other fragment.

From the archaeological point of view, considering the importance of the Antinous statue, to group the fragments that can be attributed to it constitutes a substantial achievement. The statue is the only known representation of the young Bithynian in Hispania, highlighting the singularity of the decorative program of the Els Munts villa. It is also one of the few Antinous statues with preserved head, torso, and part of the extremities. For most of the known models, only the head has been preserved, and only a few include the torso [33]. Moreover, the approach presented represents a first step to undertake a systematic archaeometric classification of the scattered marble fragments retrieved from the Els Munts villa. The work could be extended to many other fragments from the same site, contributing to reveal more data about the richness and the predominant iconography that decorated this villa, near Roman Tarraco.

The innovative use of CL and isotopic analyses to reconstruct fragmented sculptures or other artwork should be extended to other archaeological sites. This would assess the reliability of the method, and it could be established as a regular approach for sculpture reconstruction, in addition to the already common contribution of these techniques to marble provenance determination.

Supplementary Materials: The following supporting information can be downloaded at: <https://www.mdpi.com/article/10.3390/min12121614/s1>, Figure S1: Illustrative micrographs of all the analyzed samples observed in XPL. Figure S2: Illustrative micrographs of all the analyzed samples viewed under the CL microscope using an exposure time of 15 s. Figure S3: Cropped CL image areas (exposure time: 15 s) and their corresponding simplified versions obtained after application of the CLARA algorithm.

Author Contributions: Conceptualization, L.C., R.D.F. and J.C.R.; sample selection, J.C.R.; sampling, L.C., R.D.F. and J.C.R.; petrography, R.D.F. and F.A.; isotopic measurements, M.B.; cathodoluminescence (CL) measurements, L.C., R.D.F. and J.D.M.-M.; CL color clustering and quantification, L.C.; writing—original draft preparation, L.C., R.D.F. and J.C.R.; writing—review and editing, L.C., R.D.F., J.C.R., M.B., F.A. and J.D.M.-M. All authors have read and agreed to the published version of the manuscript.

Funding: This research is partially funded by the Spanish Ministry of Science and Innovation, grant numbers PID2019-104120GB-I00, PID2021-122467NB-C22, and PID2021-122879OB-I00.

Data Availability Statement: Most of the data presented in this study have been made publicly available within the Supplementary Materials section. Any other data are available on request from the corresponding author.

Acknowledgments: Mònica Borrell, Montserrat Perramon, and Josep Anton Remolà, from the Museu Nacional Arqueològic de Tarragona (MNAT) museum are recognized for granting permission to sample the studied marbles. We are thankful to Lorenzo Lazzarini for providing advice on petrographic descriptions and interpretations. Marc Anglisano is acknowledged for providing support on image-analysis tools.

Conflicts of Interest: The authors declare no conflict of interest.

References

1. Fazio, L.; lo Brutto, M.; Gonizzi Barsanti, S.; Malatesta, S.G. The Virtual Reconstruction of the Aesculapius and Hygeia Statues from the Sanctuary of Isis in Lilybaeum: Methods and Tools for Ancient Sculptures’ Enhancement. *Appl. Sci.* **2022**, *12*, 3569. [[CrossRef](#)]
2. Patay-Horváth, A. The Virtual 3D Reconstruction of the East Pediment of the Temple of Zeus at Olympia an Old Puzzle of Classical Archaeology in the Light of Recent Technologies. *Digit. Appl. Archaeol. Cult. Herit.* **2014**, *1*, 12–22. [[CrossRef](#)]
3. Palmas, G.; Pietroni, N.; Cignoni, P.; Scopigno, R. A Computer-Assisted Constraint-Based System for Assembling Fragmented Objects. In Proceedings of the 2013 Digital Heritage International Congress (DigitalHeritage), Marseille, France, 28 October–1 November 2013; Volume 1, pp. 529–536.
4. Coleman, M.; Walker, S. Stable isotope identification of greek and turkish marbles. *Archaeometry* **1979**, *21*, 107–112. [[CrossRef](#)]
5. Lapuente, P.; León, P.; Nogales, T.; Royo, H.; Preite-Martinez, M.; Blanc, P. White Sculptural Materials from Villa Adriana: Study of Provenance. In *Proceedings of the Interdisciplinary Studies on Ancient Stone. Proceedings of the IX ASMOSIA Conference*; Tarragona, Spain, 8–13 June 2009; Gutiérrez Garcia-Moreno, A., Lapuente, P., Rodà, I., Eds.; Institut Català d’ Arqueologia Clàssica: Tarragona, Spain, 2009; Volume 23, pp. 365–375.
6. Decrouez, D.; Barbin, V.; Ramseyer, K.; Maier, J.-L.; Chamay, J. Tracing of archaeological marbles by cathodoluminescence. In *Science, Technology and European Cultural Heritage*; Baer, N.S., Sabbioni, C., Eds.; Butterworth-Heinemann: Oxford, UK, 1991; pp. 591–592. ISBN 978-0-7506-0237-2.
7. Antonelli, F.; Lapuente, M.P.; Dessandier, D.; Kamel, S. Petrographic Characterization and Provenance Determination of the Crystalline Marbles Used in the Roman City of Banasa (Morocco): New Data on the Import of Iberian Marble in Roman North Africa. *Archaeometry* **2015**, *57*, 405–425. [[CrossRef](#)]
8. Pensabene, P.; Antonelli, F.; Lazzarini, L.; Cancelliere, S. Provenance of Marble Sculptures and Artifacts from the So-Called Canopus and Other Buildings of “Villa Adriana” (Hadrian’s Villa–Tivoli, Italy). *J. Archaeol. Sci.* **2012**, *39*, 1331–1337. [[CrossRef](#)]
9. Ouazaa, N.L.; Casas, L.; Álvarez, A.; Fouzai, B.; Moreno-Vide, M.; Vidal, L.; Sihem, R.; Sonzogni, C.; Borschneck, D. Provenance of Marble Sculptures from the National Museum of Carthage (Tunisia). *J. Archaeol. Sci.* **2013**, *40*, 1602–1610. [[CrossRef](#)]
10. Casas, L.; di Febo, R.; Brilli, M.; Giustini, F.; Gozzi, M.; de Caprariis, F.; Martín-Martín, J.D.; Parisi Presicce, C. Exploring New Ways to Reconstruct the Forma Urbis Romae: An Archaeometric Approach (CL Color and Stable Isotope Analyses). *Minerals* **2021**, *11*, 1400. [[CrossRef](#)]
11. Remolà, J.A. *Vil·la Romana Dels Munts (Tarraco)*; Museu Nacional Arqueològic de Tarragona/Agència Catalana de Patrimoni Cultural: Tarragona, Spain.
12. Koppel, E.M. Informe Preliminar Sobre La Decoración Escultórica de La Villa Romana de ‘Els Munts’ (Altafulla, Tarragona). *Madr. Mitt.* **2000**, *41*, 380–394.
13. Koppel, E.M. La Decoración Escultórica: Esculturas Exentas. In *Vil·la Romana dels Munts (Tarraco)*; Remolà, J.A., Ed.; Museu Nacional Arqueològic de Tarragona/Agència Catalana de Patrimoni Cultural: Tarragona, Spain.
14. Ruiz, J.C. Escultura Decorativa y Estatuas Fragmentadas. In *Vil·la Romana dels Munts (Tarraco)*; Remolà, J.A., Ed.; Museu Nacional Arqueològic de Tarragona/Agència Catalana de Patrimoni Cultural: Tarragona, Spain.
15. Mayer, M.; Álvarez, A. Le Marbre Grec Comme Indice Pour Les Pieces Sculpturiques Grecques Ou de Tradition Grecque En Espagne. In Proceedings of the XII Congrès International d’Archéologie, Athènes, Greece, 4–10 September 1983; Hypourgeio Politismou kai Epistemon: Athens, Greece, 1984; pp. 184–190.
16. Pensabene, P. Mármoles y Talleres En La Bética y Otras Áreas de La Hispania Romana. In *El Concepto de lo Provincial en el Mundo Antiguo: Homenaje a la Profesora Pilar León Alonso*; Vaquerizo, D., Murillo, J.F., Eds.; Universidad de Córdoba: Córdoba, Spain, 2006; pp. 103–142.
17. Kaufman, L.; Rousseeuw, P.J. *Finding Groups in Data: An Introduction to Cluster Analysis*; John Wiley & Sons, Inc.: New York, NY, USA, 1990.
18. Burkhard, M. Calcite Twins, Their Geometry, Appearance and Significance as Stress-Strain Markers and Indicators of Tectonic Regime: A Review. *J. Struct. Geol.* **1993**, *15*, 351–368. [[CrossRef](#)]
19. Antonelli, F.; Lazzarini, L. An Updated Petrographic and Isotopic Reference Database for White Marbles Used in Antiquity. *Rend. Lincei* **2015**, *26*, 399–413. [[CrossRef](#)]
20. Lapuente, M.P.; Turi, B.; Blanc, P. Marbles from Roman Hispania: Stable Isotope and Cathodoluminescence Characterization. *Appl. Geochem.* **2000**, *15*, 1469–1493. [[CrossRef](#)]
21. Boggs, S.; Krinsley, D. *Application of Cathodoluminescence Imaging to the Study of Sedimentary Rocks*; Cambridge University Press: Cambridge, UK, 2006.

22. Habermann, D.; Neuser, R.D.; Richter, D.K. Low Limit of Mn²⁺-Activated Cathodoluminescence of Calcite: State of the Art. *Sediment. Geol.* **1998**, *116*, 13–24. [[CrossRef](#)]
23. Hiatt, E.; Pufahl, P. Cathodoluminescence Petrography of Carbonate Rocks: A Review of Applications for Understanding Diagenesis, Reservoir Quality, and Pore System Evolution. In *Cathodoluminescence and Its Application to Geoscience*; Coulson, I., Ed.; Mineralogical Association of Canada: Québec, QC, Canada, 2014; pp. 75–96.
24. Machel, H.G. *Application of Cathodoluminescence to Carbonate Diagenesis BT-Cathodoluminescence in Geosciences*; Pagel, M., Barbin, V., Blanc, P., Ohnenstetter, D., Eds.; Springer: Berlin/Heidelberg, Germany, 2000; pp. 271–301; ISBN 978-3-662-04086-7.
25. Barbin, V.; Ramseyer, K.; Fontignie, D.; Burns, S.; Decrouez, D. Differentiation of Blue-Cathodoluminescing White Marbles. In *Ancient Stones: Quarrying, Trade and Provenance. Katholieke Universiteit Leuven. Acta Archaeologica Lovaniensia, Monographiae 4*; Waelkens, M., Herz, N., Moens, L., Eds.; Leuven University Press: Leuven, Belgium, 1992; pp. 231–236.
26. Barbin, V.; Ramseyer, K.; Decrouez, D.; Burns, S.; Chamay, J.; Maier, J. Cathodoluminescence of White Marbles: An Overview. *Archaeometry* **1992**, *34*, 175–183. [[CrossRef](#)]
27. Lapuente, P.; Rodà, I.; Gutiérrez Garcia-M, A.; Brilli, M. Addressing the Controversial Origin of the Marble Source Used in the Phoenician Anthropoid Sarcophagi of Gadir (Cadiz, Spain). *Archaeometry* **2021**, *63*, 467–480. [[CrossRef](#)]
28. Blanc, P.; Lapuente Mercadal, M.P.; Gutiérrez Garcia-Moreno, A. A New Database of the Quantitative Cathodoluminescence of the Main Quarry Marbles Used in Antiquity. *Minerals* **2020**, *10*, 381. [[CrossRef](#)]
29. Wielgosz-Rondolino, D.; Antonelli, F.; Bojanowski, M.J.; Gładki, M.; Göncüoğlu, M.C.; Lazzarini, L. Improved Methodology for Identification of Göktepe White Marble and the Understanding of Its Use: A Comparison with Carrara Marble. *J. Archaeol. Sci.* **2020**, *113*, 105059. [[CrossRef](#)]
30. Antonelli, F.; Lazzarini, L. The Use of White Marble in the Central and Upper Adriatic Between Greece and Rome: Hellenistic Stelae from the Necropolis of Ancona (Italy). *Camb. Archaeol. J.* **2013**, *23*, 149–162. [[CrossRef](#)]
31. Barbin, V.; Ramseyer, K.; Decrouez, D.; Herb, R. Marbres Blancs: Caractérisation Par Cathodoluminescence. *Comptes Rendus De L'Académie Des Sci. Paris (II)* **1989**, *308*, 861–866.
32. Gravesen, J. The Metric of Colour Space. *Graph. Model.* **2015**, *82*, 77–86. [[CrossRef](#)]
33. Meyer, H. *Antinoos: Die Archäologischen Denkmäler Unter Einbeziehung Des Numismatischen Und Epigraphischen Materials Sowie Der Literarischen Nachrichten. Ein Beitrag Zur Kunst- Und Kulturgeschichte Der Hadrianisch-Frühantoninischen Zeit*; Brill: Munich, Germany, 1991; ISBN 978-3-7705-2634-5.